

TRANSPORT OF TOROIDAL MAGNETIC FIELD BY THE MERIDIONAL FLOW AT THE BASE OF THE SOLAR CONVECTION ZONE

MATTHIAS REMPEL

High Altitude Observatory, National Center for Atmospheric Research* , P.O. Box 3000, Boulder, Colorado 80307, USA

Draft version June 26, 2021

ABSTRACT

In this paper we discuss the transport of toroidal magnetic field by a weak meridional flow at the base of the convection zone. We utilize the differential rotation and meridional flow model developed by Rempel and incorporate feedback of a purely toroidal magnetic field in two ways: directly through the Lorentz force (magnetic tension) and indirectly through quenching of the turbulent viscosity, which affects the parameterized turbulent angular momentum transport in the model. In the case of direct Lorentz force feedback we find that a meridional flow with an amplitude of around 2 ms^{-1} can transport a magnetic field with a strength of 20 kG to 30 kG. Quenching of turbulent viscosity leads to deflection of the meridional flow from the magnetized region and a significant reduction of the transport velocity if the magnetic field is above equipartition strength.

Subject headings: Sun: interior — rotation — magnetic field — dynamo

1. INTRODUCTION

Flux-transport dynamos have proven to be successful for modeling the evolution of the large scale solar magnetic field (Choudhuri et al. 1995; Dikpati & Charbonneau 1999). In a flux-transport dynamo the equatorward propagation of the magnetic activity belt (butterfly diagram) is a consequence of the equatorward transport of magnetic field at the base of the convection zone by the meridional flow.

However, all studies so far addressed the transport of magnetic field by the meridional circulation in a purely kinematic regime. The toroidal field strength at the base of the solar convection zone inferred from studies of rising magnetic flux tubes (Choudhuri & Gilman 1987; Fan et al. 1993; Schüssler et al. 1994; Caligari et al. 1995, 1998) is around 100 kG and thus orders of magnitude larger than the equipartition field strength estimated from a meridional flow velocity of a few ms^{-1} . Therefore it is crucial for flux-transport dynamos to address the feedback of the Lorentz force on the meridional flow.

In order to be able to address this question it is necessary to incorporate a model for the solar differential rotation and meridional flow into a dynamo model and allow for the feedback of the Lorentz force on differential rotation and meridional flow. Differential rotation and meridional flow have been addressed in the past through mainly two approaches: 3D full spherical shell simulations (Glatzmaier & Gilman 1982; Gilman & Miller 1986; Miesch et al. 2000; Brun & Toomre 2002) and axisymmetric mean field models (Kitchatinov & Rüdiger 1993, 1995; Rüdiger et al. 1998; Küker & Stix 2001). While the 3D simulations have trouble reproducing a consistent large scale meridional flow pattern (poleward in the upper half of the convection zone), as it is observed by helioseismology (Braun & Fan 1998; Haber et al. 2002; Zhao & Kosovichev 2004), such a flow is a common feature in most of the mean field models.

In this paper we present a first step toward building a dynamical dynamo model by focusing primarily on the transport of a prescribed toroidal magnetic field by meridional circulation. We do not attempt in this very first model to solve the dynamo equations in order to generate the magnetic fields. To this end we will use the mean field model for differential rotation and meridional circulation described by Rempel (2005) and extend it by incorporating the magnetic tension resulting from a purely toroidal magnetic field at the base of the solar convection zone. In this paper we assume that the toroidal magnetic field consists of a homogeneous layer. We will briefly discuss in section 2 how an intermittent field structure will change the results. In a future paper we will present a full axisymmetric mean field dynamo simulation.

2. MODEL

In this paper we utilize the differential rotation / meridional circulation model of Rempel (2005) and add the Lorentz force of a toroidal magnetic field. For the details of the model we refer to Rempel (2005). The equations we solve are:

$$\frac{\partial \varrho_1}{\partial t} = -\frac{1}{r^2} \frac{\partial}{\partial r} (r^2 v_r \varrho_0) - \frac{1}{r \sin \theta} \frac{\partial}{\partial \theta} (\sin \theta v_\theta \varrho_0) \quad (1)$$

$$\begin{aligned} \frac{\partial v_r}{\partial t} = & -v_r \frac{\partial v_r}{\partial r} - \frac{v_\theta}{r} \frac{\partial v_r}{\partial \theta} + \frac{v_\theta^2}{r} - \frac{\partial}{\partial r} \frac{p_{\text{tot}}}{\varrho_0} + \frac{p_{\text{mag}}}{\gamma p_0} g + \frac{s_1}{\gamma} g \\ & + (2\Omega_0 \Omega_1 + \Omega_1^2) r \sin^2 \theta + \frac{F_r}{\varrho_0} - \frac{B^2}{\mu_0 \varrho_0 r} \quad (2) \end{aligned}$$

$$\begin{aligned} \frac{\partial v_\theta}{\partial t} = & -v_r \frac{\partial v_\theta}{\partial r} - \frac{v_\theta}{r} \frac{\partial v_\theta}{\partial \theta} - \frac{v_r v_\theta}{r} - \frac{1}{r} \frac{\partial}{\partial \theta} \frac{p_{\text{tot}}}{\varrho_0} \\ & + (2\Omega_0 \Omega_1 + \Omega_1^2) r \sin \theta \cos \theta + \frac{F_\theta}{\varrho_0} \\ & - \frac{B^2}{\mu_0 \varrho_0 r} \cot \theta \quad (3) \end{aligned}$$

$$\frac{\partial \Omega_1}{\partial t} = -\frac{v_r}{r^2} \frac{\partial}{\partial r} [r^2 (\Omega_0 + \Omega_1)]$$

*The National Center for Atmospheric Research is sponsored by the National Science Foundation
 Electronic address: rempel@hao.ucar.edu

$$-\frac{v_\theta}{r \sin^2 \theta} \frac{\partial}{\partial \theta} [\sin^2 \theta (\Omega_0 + \Omega_1)] + \frac{F_\phi}{\varrho_0 r \sin \theta} \quad (4)$$

$$\begin{aligned} \frac{\partial s_1}{\partial t} = & -v_r \frac{\partial s_1}{\partial r} - \frac{v_\theta}{r} \frac{\partial s_1}{\partial \theta} + v_r \frac{\gamma \delta}{H_p} + \frac{\gamma - 1}{p_0} Q \\ & + \frac{1}{\varrho_0 T_0} \nabla \cdot (\kappa_t \varrho_0 T_0 \nabla s_1) \end{aligned} \quad (5)$$

where

$$p_{\text{mag}} = \frac{B^2}{2\mu_0} \quad (6)$$

$$p_{\text{tot}} = p_1 + p_{\text{mag}} \quad (7)$$

$$H_p = \frac{p_0}{\varrho_0 g} \quad (8)$$

p_1 denotes the pressure perturbation with respect to the reference state, p_0 , and s_1 is the entropy perturbation $s_1 = p_1/p_0 - \gamma \varrho_1/\varrho_0$ (made dimensionless with the heat capacity c_v), where ϱ_0 denotes the density of the reference state. We use a reference state corresponding to a polytropic atmosphere with gravity varying $\sim r^{-2}$. Since our model describes the convection zone and overshoot region where the deviation from adiabaticity are small ($|\nabla - \nabla_{\text{ad}}| \ll 1$) we use an adiabatic polytrope for the reference state. However small perturbations from adiabaticity are considered in the entropy equation Eq. (5) through the third term on the right hand side. We use values for $\delta = \nabla - \nabla_{\text{ad}} \sim -10^{-5}$ below $r = 0.725 R_\odot$ and $\delta = 0$ above. Different profiles of δ influence primarily the differential rotation profile (more specific: the deviation from the Taylor-Proudman state); however, the influence on the meridional flow, which is of primary interest here, is very weak. Ω_0 denotes the core rotation rate. κ_t in Eq. (5) denotes the turbulent convective heat diffusivity and Q the viscous heating. We write the pressure/buoyancy term in Eq. (2) assuming small deviations from adiabaticity ($|\nabla - \nabla_{\text{ad}}| \ll 1$).

F_r , F_θ , and F_ϕ denote the viscous stress including a parameterization of turbulent angular momentum transport (Λ -effect, Kitchatinov & Rüdiger (1995)). The turbulent angular momentum transport is the driver for the differential rotation and the meridional flow in this model. The exact form of these terms is discussed in detail in Rempel (2005).

In this model we do not include the induction equation, which would be required to address the non-linear evolution of the field transported by the meridional flow. As a first step towards the full problem we solve here for a stationary solution similar to Rempel (2005), but include the magnetic tension force of a toroidal magnetic field. This allows determination of the field strength up to which an equatorward transport of toroidal magnetic field is possible if the feedback of the magnetic tension force on the meridional flow is included. For reasons of simplicity, we omit the magnetic buoyancy term in Eq. (2) (fifth term on right-hand side) and focus this discussion only on the magnetic tension force. Magnetic buoyancy has been addressed in great detail by Moreno-Insertis et al. (1992) and Rempel et al. (2000).

In this study we assume a homogeneous toroidal field at the base of the convection zone. Alternatively the magnetic field could be highly intermittent leading to the following two complications: The Lorentz force is dependent on the structure of the field in detail and cannot

be expressed just by the mean field alone; the advection velocity of the mean field is not given by the mean flow, since field free plasma can flow around magnetic elements. In that sense for the case of intermittent field there are two extreme scenarios possible: 1. The field is highly intermittent and couples only weakly through the drag force of individual flux elements to the mean flow. In this case the equatorward transport of field by the meridional flow is mainly dependent on the strength of the coupling between mean field and mean flow (similar to the behavior of individual flux tubes as discussed by Rempel (2003)); the change of the meridional flow pattern by the feedback of the Lorentz force is a secondary effect. 2. The coupling between mean flow and mean field is strong. In this case equatorward transport of field by the meridional flow is dependent on the change of the meridional flow pattern caused by the Lorentz force.

Even though we assume a homogeneous field in this study, our results also apply to intermittent field in the case of strong coupling discussed above. Independent from the particular way the field couples to the fluid, momentum conservation requires that the bulk force acting on the bulk flow is given by the mean Lorentz force. However, the relation between the mean Lorentz force and the mean field strength can be more complicated as we illustrate in the following very simple example.

Assume the toroidal field consists of magnetic flux elements with total filling factor f and field strength B_0 . The mean tension force $\langle F_t \rangle$ is proportional to $f B_0^2$, while the mean field strength is given by $\langle B \rangle = f B_0$, therefore $\langle F_t \rangle \sim \langle B \rangle^2 / f$. This means that for a given tension force the assumption of an intermittent field requires a factor of $f^{1/2}$ smaller mean field compared to the homogeneous case; however the field strength of individual flux elements would be a factor $f^{-1/2}$ larger.

In this paper we evaluate under which conditions an equatorward meridional flow at the base of the convection zone can transport magnetic field equatorward. To this end we compute at a fixed latitude the following effective transport velocity for a given magnetic field configuration:

$$v_\theta^{\text{eff}} = \frac{\int v_\theta B r dr}{\int B r dr}, \quad (9)$$

where $v_\theta^{\text{eff}} > 0$ means a transport of magnetic flux toward the equator. In the case of intermittent field v_θ^{eff} will be an upper estimate for the transport capability. Explicitly calculating the coupling between mean flow and mean field is beyond the scope of this paper and most likely highly dependent on the exact field configuration.

3. NUMERICAL RESULTS

In this section we use models for the differential rotation and meridional flow which are very similar to model 1 in Rempel (2005). Parameters that differ from those used in Rempel (2005) are summarized in Tab. 1. We have chosen the parameters such that we have three models with meridional flow velocities varying by a factor of 4, while the turbulent diffusivity is unchanged (model 1, 2, 3) and three models with a turbulent diffusivity varying by a factor of 4, while the meridional flow speed is roughly the same (model 1, 4, 5). Fig. 1 shows the flow profile of v_θ at 30° latitude for the models listed in Tab. 1.

TABLE 1
PARAMETERS OF REFERENCE MODELS

model	Λ_0	λ [°]	κ_t, ν_t [m ² s ⁻¹]
1	0.8	15	$5 \cdot 10^8$
2	1.49	7.5	$5 \cdot 10^8$
3	0.43	22.5	$5 \cdot 10^8$
4	1.36	7.5	$2.5 \cdot 10^8$
5	0.48	22.5	10^9

NOTE. — Parameters of differential rotation models used. Models 1 to 3 show different meridional flow velocities for the same value of the turbulent diffusivity, whereas models 1, 4, and 5 show roughly the same meridional flow velocity for different values of the turbulent diffusivity. The parameter Λ_0 determines the amplitude of the turbulent angular momentum flux, the parameter λ the direction of the angular momentum flux with respect to the axis of rotation. The quantities κ_t and ν_t denote turbulent thermal diffusivity and turbulent viscosity, respectively.

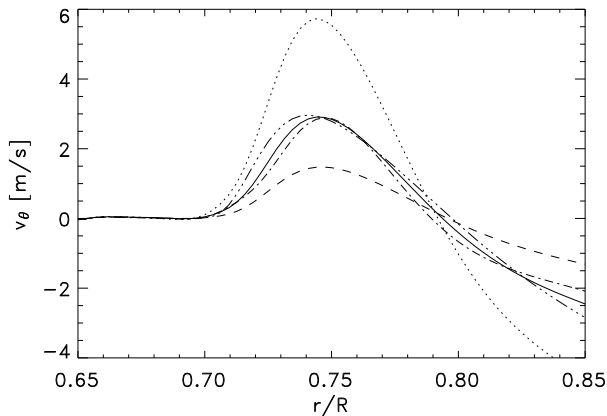


FIG. 1.— Meridional flow velocity of the reference models listed in Table 1. Shown is a radial cut of the θ velocity at 30° latitude of model 1 (solid), model 2 (dotted), model 3 (dashed), model 4 (dashed-dotted), and model 5 (dashed-triple-dotted). Models 1–3 have the same turbulent viscosity but different flow velocities, while models 4 and 5 have similar flow velocities as model 1, but different turbulent viscosities.

Fig. 2 summarizes the results obtained with the reference models 1, 2, and 3 (varying flow speed, but same turbulent viscosity). It turns out that the changes of the meridional flow and differential rotation are largely independent of the reference model (within a few percent variation). Therefore we plot in Fig. 2 a) and b) the change of meridional flow and differential rotation for the reference model 1. In each case we add magnetic field with a maximum strength of 1 T, 2 T, 3 T, and 4 T. The magnetic field is located at 30° latitude and has a radial width of $0.05 R_\odot$ and a parabolic profile in B^2 that is centered at $0.75 R_\odot$. In latitude we use a Gaussian profile with a width of about 15° . For the case with 4 T field strength the change of meridional flow speed has a maximum amplitude of around 7 m s^{-1} and is therefore larger than the meridional flow to be expected at the base of the convection zone (the observed surface flow speed is

around $10 - 20 \text{ m s}^{-1}$, which requires only a return flow of $1 - 2 \text{ m s}^{-1}$ at the base of the convection zone due to mass conservation).

A consequence of the meridional flow change induced by the magnetic tension force is the formation of a prograde jet within the magnetized region shown in Fig. 2 b), which partially compensates the magnetic tension due to the Coriolis force. The amplitude of the jet that would be required for a complete compensation is given by (see section 4 for a derivation):

$$\frac{\Omega'_1}{\Omega_0} = \frac{1}{2} \left(\frac{v_a}{\Omega_0 r \sin \theta} \right)^2, \quad (10)$$

with the Alfvén speed $v_a = B/\sqrt{\mu_0 \rho}$. For a field of 4 T at $r = 0.75 R_\odot$, 30° latitude, and value of $\rho_0 = 150 \text{ kg m}^{-3}$ this yields $\Omega'_1/\Omega_0 \approx 0.025$, which means that for the case shown in Fig 2 the jet compensates about 70% of the magnetic tension force (for the other field strengths shown, this ratio is about the same).

The interesting result is that the prograde jet forms independent of whether the magnetic field is transported equatorward or poleward (angular momentum conservation would only provide a prograde jet for a poleward movement). This is caused by the fact that the reference state (without any influence of magnetic field) is characterized by an equilibrium between turbulent angular momentum transport (including dissipative terms and non dissipative terms "Λ-effect") and the angular momentum transport of the meridional flow (the divergence of the total angular momentum flux has to be zero for a stationary solution). The magnetic tension force reduces the equatorward flow speed at the base of the convection zone, disturbing this balance and therefore forcing a change of the differential rotation. Formally this result can be understood as follows: Let \mathbf{F}_Λ^0 , \mathbf{F}_ν^0 , and \mathbf{F}_m^0 be the angular momentum fluxes in the reference state due to turbulent non-dissipative angular momentum transport (Λ-effect), turbulent dissipation, and meridional flow, respectively. Then the stationary reference state is characterized by $\nabla \cdot (\mathbf{F}_\Lambda^0 + \mathbf{F}_\nu^0 + \mathbf{F}_m^0) = 0$. The presence of a magnetic field changes the meridional flow, leading to a perturbation \mathbf{F}_m^1 , which changes the differential rotation and leads to a perturbation of the dissipative angular momentum flux \mathbf{F}_ν^1 . Since the Λ-effect remains unaffected in this case, the new stationary equilibrium requires $\nabla \cdot (\mathbf{F}_m^1 + \mathbf{F}_\nu^1) = 0$. Since for all cases considered \mathbf{F}_m^1 is always poleward directed in the magnetized region, this requires the formation of a prograde jet, even though $\mathbf{F}_m^0 + \mathbf{F}_m^1$ can be still equatorward directed.

Moreno-Insertis et al. (1992); Rempel et al. (2000) discussed the formation of prograde jets required for equilibrium states of toroidal field at the base of the convection zone. In their studies a poleward movement of the magnetic field was always required, since turbulent angular momentum transport and meridional flow were not considered in the reference state. The magnetic field strength of around 10 T they considered is also significantly larger than the field strength we will focus on in this paper.

While the changes of the meridional flow are independent of the meridional flow speed in the reference model, the question whether magnetic field is still transported

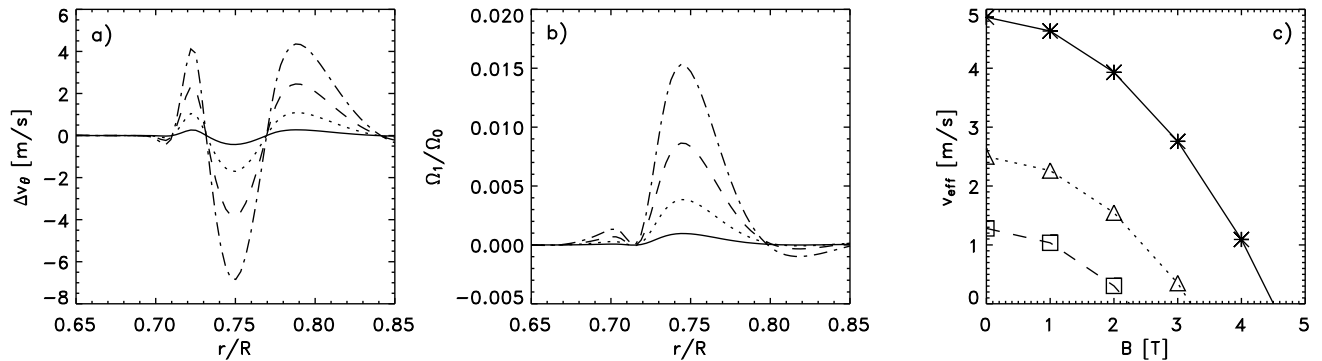


FIG. 2.— Panel a): Changes of the meridional flow resulting from the presence of a toroidal field with an amplitude of 1 T (solid), 2 T (dotted), 3 T (dashed), and 4 T (dashed-dotted). The solutions shown here use the reference model 1; however, models 2 and 3 show a very similar flow pattern (the differences are of the order of a few percent). Panel b) shows the change of differential rotation. The presence of a magnetic field leads to the formation of a prograde flow within the magnetized region. The amplitude of this jet is strong enough to compensate around 70% of the magnetic tension force through the resulting Coriolis force. Panel c) shows the effective transport velocity computed from Eq. (9) as function of field strength. Shown are the results for the reference models 1 (triangles), 2 (asterisks), and 3 (squares).

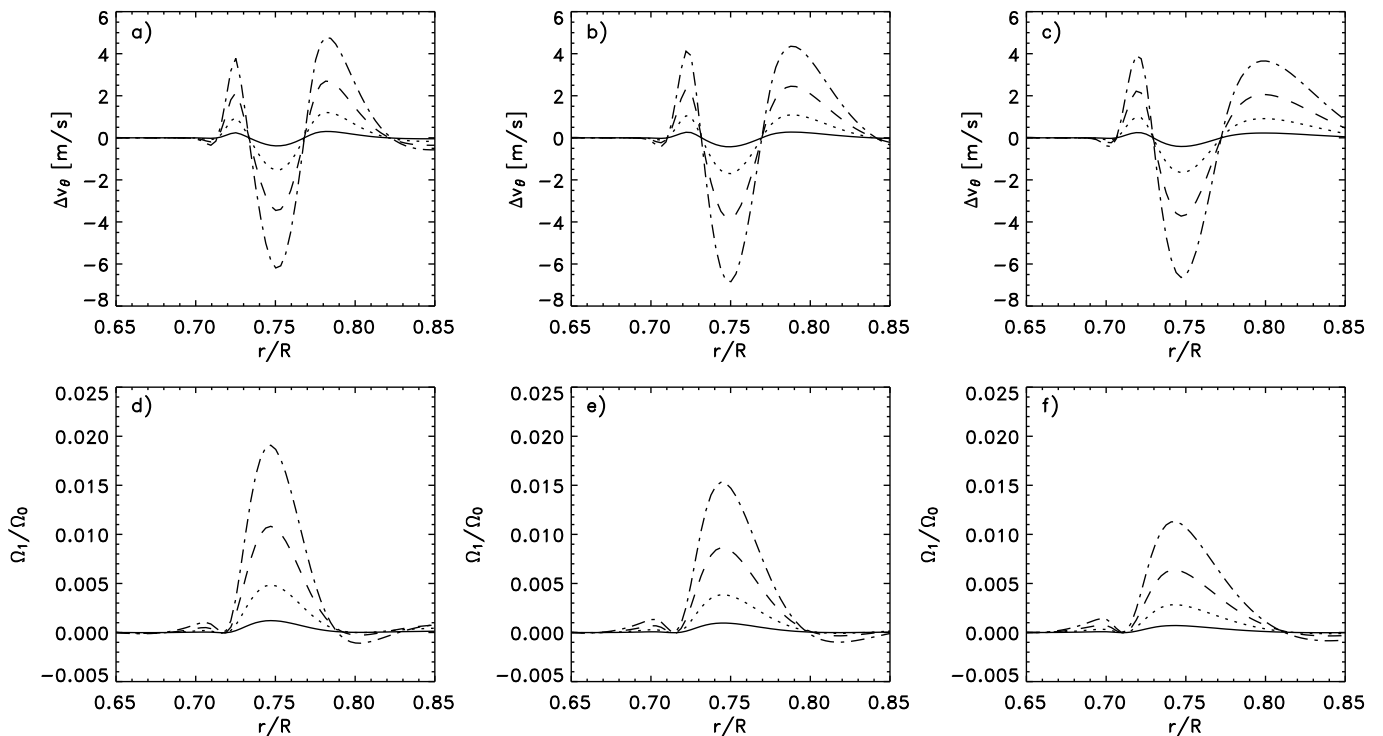


FIG. 3.— Changes of meridional flow (top) and differential rotation (bottom) using the reference models 4, 1, and 5 (left to right). An increase of turbulent viscosity (left to right) while keeping the flow speed constant leads to a spread of the side lobes and a reduction of the prograde flow within the magnetized region. The linestyle indicates different magnetic field strength as in Fig. 2. The effective transport velocity is only marginally affected (see Fig. 5).

equatorward depends on the total flow speed. Fig. 2 c) shows the effective transport velocity according to Eq. (9) for the three cases. In the case of a meridional flow of around 1.5 m s^{-1} , magnetic fields up to about 2.2 T can be transported equatorward, while a 6 m s^{-1} flow could transport up to 4.5 T equatorward. Note that the critical field strength scales roughly with the square-root of the meridional flow velocity. This is different from the case of individual flux tubes coupling to the flow through the drag force, which results in $B \sim v$.

Fig. 3 shows the result for reference models 1, 4, and

5 that have roughly the same flow velocity, but a variation in the turbulent viscosity by a factor of 4. Even though the amplitude of the prograde jet changes significantly, the transport capability of the meridional flow (see Fig. 5) is only marginally affected. In the model 4 with a value of $\nu_t = 2.5 \cdot 10^8 \text{ m}^2 \text{ s}^{-1}$ the jet compensates around 90% of the curvature force (left panels), whereas in model 5 with a value of $\nu_t = 10^9 \text{ m}^2 \text{ s}^{-1}$ the jet compensates only around 50% of the curvature force (right panels). This does not affect strongly the transport capability of the meridional flow since at the same time with

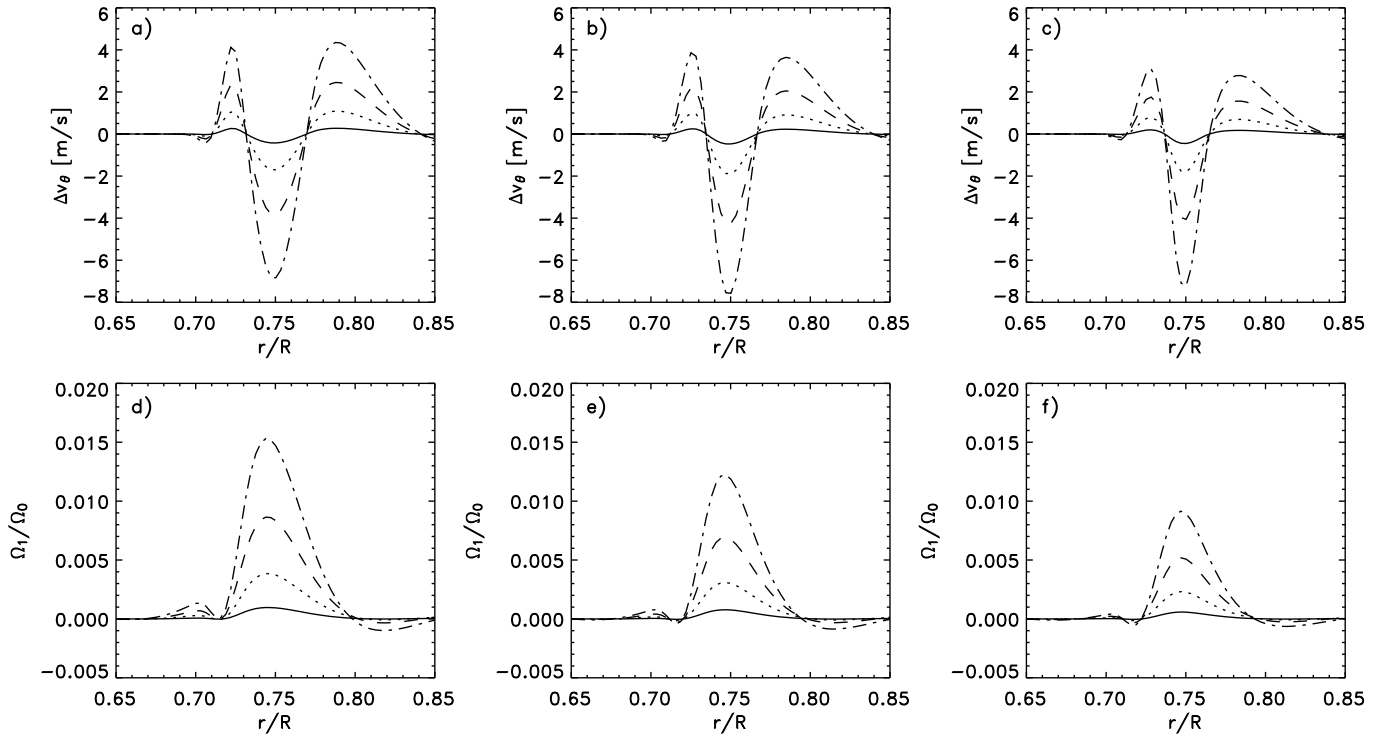


FIG. 4.— Changes of meridional flow (top) and differential rotation (bottom) using the reference models 1 and a decreasing width of the magnetic field profile. The width of the field profile centered at $r = 0.75R_{\odot}$ decreases from $0.05R_{\odot}$ to $0.025R_{\odot}$ (left to right). Similar to the increase of turbulent viscosity, a decrease of width leads to a reduction of the prograde flow within the magnetized region. The linestyle indicates different magnetic field strength as in Fig. 2. The effective transport velocity is only marginally affected (see Fig. 5).

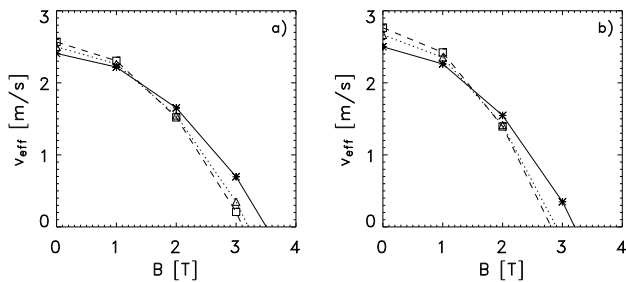


FIG. 5.— Effective transport velocity for the cases shown in Fig. 3 (left) and Fig. 4 (right). Asterisks, triangles, squares correspond to the solutions shown in Fig. 3 and 4 on the left, middle, right, respectively.

increasing turbulent viscosity the transport of magnetic field through viscous drag increases (a typical value of the Reynolds number on scales of the magnetic field is of the order of one due to the small meridional flow velocity and the large turbulent viscosity). We will discuss this in detail in section 4.

Fig. 4 shows the result for different radial widths of the magnetic field. In all cases we use model 1 as the reference model. Panels a) and d) show results for a width of $0.05R_{\odot}$, panels b) and e) for a width of $0.035R_{\odot}$, and panels c) and f) for a width of $0.025R_{\odot}$. A comparison with Fig. 3 shows clearly that a reduction of the width of the magnetic field is equivalent to an increase of the viscosity as expected from a simple scaling argument.

Fig. 5 shows the effective transport velocity for the

cases shown in Fig. 3 (left panel) and Fig. 4 (right panel). Changes of the turbulent viscosity (by a factor of 4) and the width of the magnetic field (by a factor of 2) considered here influence the critical field strength up to which an equatorward transport of flux is possible by around 10%.

4. ANALYTIC ESTIMATE

Let v_r , v_{θ} , and Ω_1 be a stationary solution of the differential rotation problem without a magnetic field, and v'_r , v'_θ , and Ω'_1 perturbations around that state caused by the presence of the magnetic field. Only considering the θ -component of the momentum equation, we can estimate the balance between Coriolis force, magnetic tension and viscous stress by:

$$2\Omega_0\Omega'_1 r \sin\theta \cos\theta - \frac{B^2}{\mu_0 \rho_0 r} \cot\theta - c_d \nu_t \frac{v'_\theta}{d^2} = 0, \quad (11)$$

where d denotes a length associated with the radial width of the magnetic field and c_d is a coefficient, which takes care of the more complicated flow structure. The formulation given here relates to the more general formulation of the drag force $\sim c_w \rho v^2 / (2d)$ through the assumption $c_w \sim c_d / Re$ with the turbulent Reynolds number $Re = v d / \nu_t$. Since the large scale flow pattern in combination with the large turbulent viscosity is a flow with a small turbulent Reynolds number ~ 1 , it can be expected that the meridional flow behaves like a highly viscous fluid. This is justified as long as the scale of the flow field is larger than the typical turbulence scale. In this limit typical values for c_d should be of the order of 10 (see text books on fluid dynamics for Stokes law). For

small magnetic flux tubes a formulation with $c_w = \text{const}$ rather than $c_d = \text{const}$ is more valid. We show later that for a reasonable choice of c_d a good agreement between this analytic scaling analysis and the numerical result can be achieved.

We emphasize that drawing parallels between laminar, viscous laboratory flows and highly turbulent astrophysical flows with a low turbulent Reynolds number is speculative; however it is unavoidable when applying the mean field approach, leading to the parameterization of large turbulent viscosities.

The balance between angular momentum transport and viscous dissipation yields:

$$-2\Omega_0 \frac{v'_\theta}{r} \cot \theta - \nu_t \frac{\Omega'_1}{d^2} = 0 \quad (12)$$

We did not introduce here an additional free parameter in front of the diffusive loss term, since this prefactor ~ 1 can be easily absorbed into the definition of the length scale d . Combining both equations gives a relation between B and v'_θ :

$$B^2 = -\mu_0 \varrho_0 r \tan \theta \left((2\Omega_0 \cos \theta)^2 \frac{d^2}{\nu_t} + c_d \frac{\nu_t}{d^2} \right) v'_\theta \quad (13)$$

An equatorward transport of the magnetic field requires $|v'_\theta| \lesssim |v_\theta|$, which yields an upper limit for magnetic field strength of:

$$B^2 \sim \mu_0 \varrho_0 r \tan \theta \left((2\Omega_0 \cos \theta)^2 \frac{d^2}{\nu_t} + c_d \frac{\nu_t}{d^2} \right) v_\theta \quad (14)$$

The importance of the two terms in the angular brackets depends on the value of the turbulent viscosity ν_t and the width of the magnetic field d . For a given width, the first term is important for low viscosity, the second one for high viscosity. Both are of the same importance if

$$\nu_t = \nu_{\text{crit}} = \frac{2}{c_d^{1/2}} \Omega_0 d^2 \cos \theta. \quad (15)$$

Eq. (14) can be written together with Eq. (15) in the form:

$$B \sim 2^{1/2} c_d^{1/4} \sqrt{\mu_0 \varrho_0 \Omega_0 r \sin \theta v_\theta} \sqrt{\frac{\nu_{\text{crit}}}{\nu_t} + \frac{\nu_t}{\nu_{\text{crit}}}} \quad (16)$$

Eq. (15) shows clearly the relation $B \sim v_\theta^{1/2}$ as suggested by Fig. 2c.

Inserting Eq. (13) into Eq. (12) yields for the perturbation of Ω :

$$\frac{\Omega'_1}{\Omega_0} = \frac{1}{2} \left(\frac{v_a}{\Omega_0 r \sin \theta} \right)^2 \left[1 + \left(\frac{\nu_t}{\nu_{\text{crit}}} \right)^2 \right]^{-1} \quad (17)$$

In the case of very low viscosity the perturbation of Ω is given by

$$\frac{\Omega'_1}{\Omega_0} = \frac{1}{2} \left(\frac{v_a}{\Omega_0 r \sin \theta} \right)^2, \quad (18)$$

which is exactly the value required to balance the magnetic tension through the Coriolis force. In the case of large viscosity the Coriolis force is unimportant and the magnetic field is dragged by the meridional flow through viscous coupling.

In order to compare these estimates to the numerical results we use the model 1, which is shown in Fig. 2 panels a) and b). As already mentioned earlier the jet amplitude is sufficient to compensate for 70% of the curvature stress, which yields according to Eq. (17) $\nu_t \sim 0.65 \nu_{\text{crit}}$. With a value of $\nu_t \sim 2.5 \cdot 10^8 \text{m}^2 \text{s}^{-1}$ at $0.75 R_\odot$ (roughly half the convection zone value) and $\Omega_0 = 2.7 \cdot 10^{-6} \text{s}^{-1}$ Eq. (15) yields $d = c_d^{1/4} 0.014 R_\odot$. Using a value of $c_d = 10$ yields $d = 0.025 R_\odot$, which is half of assumed width of the magnetic field. With $c_d = 10$, $\nu_t \sim 0.65 \nu_{\text{crit}}$, $\varrho_0 = 150 \text{kg m}^{-3}$, $r = 0.75 R_\odot$, and $v_\theta \sim 2.5 \text{m s}^{-1}$ Eq. (16) yields $B \sim 2.8 \text{T}$, which is very close to the numerical result.

Since Eq. (16) as function of ν_t/ν_{crit} has a local minimum for $\nu_t = \nu_{\text{crit}}$, the dependence of B on ν_t and d (through ν_{crit} , Eq. (15)) is expected to be rather weak, whereas Ω'_1/Ω_0 shows a much stronger dependence as found in Figs. 3 and 4. In more detail, Eq. (17) does not exactly reflect the scaling of Ω'_1/Ω_0 with ν_t and d found in Figs. 3 and 4, which suggests that c_d is depending on ν_t and d itself, however the tendency is indicated correctly.

5. SOLUTIONS WITH QUENCHED VISCOSITY

So far we have discussed the back-reaction of toroidal field on the meridional low through the magnetic curvature force. Since the equipartition field strength at the base of the convection zone is around 1 T (based on mixing-length models) the magnetic field also quenches the turbulent viscosity to some extent. Since this also changes the turbulent angular momentum flux an influence on the meridional flow is expected. In order to demonstrate this effect use a very weak field of 1 T field strength, which has nearly no influence on the meridional flow through the tension force, and include a quenching of the viscosity given by

$$\nu'_t = \nu_t \left[1 + \left(\frac{B}{B_{\text{eq}}} \right)^2 \right]^{-1}. \quad (19)$$

Note that ν_t scales in our model the viscous stress and the turbulent angular momentum transport (Λ -effect). Fig. 5 a) shows the results for a the values $B_{\text{eq}} = B_{\text{max}}$, $B_{\text{eq}} = B_{\text{max}}/\sqrt{3}$, and $B_{\text{eq}} = B_{\text{max}}/\sqrt{7}$ that correspond to a quenching by a factor of 2, 4, and 8, respectively. A comparison with the results presented in Figs. 2 to 4 shows that the back-reaction through quenching of viscosity has, at least for weak field, a much stronger effect than the direct feedback through magnetic tension. Whereas in the case of feedback through magnetic tension the meridional flow moves around the magnetized region on both sides (below and above), in the case of quenching the meridional flow closes above the magnetized region. The changes of the differential rotation (panel b) are around one order of magnitude lower than in Figs. 2 to 4 and no distinct jet forms.

This results from the fact that the change in the viscosity changes the parametrized turbulent angular momentum transport that is the indirect driver for the meridional flow. In our model the meridional return flow is localized in the region where the turbulent viscosity shows the strongest radial gradient. The quenching of the viscosity moves therefore the return flow upward, as clearly indicated in Fig. 6 panel c). However, the transport of

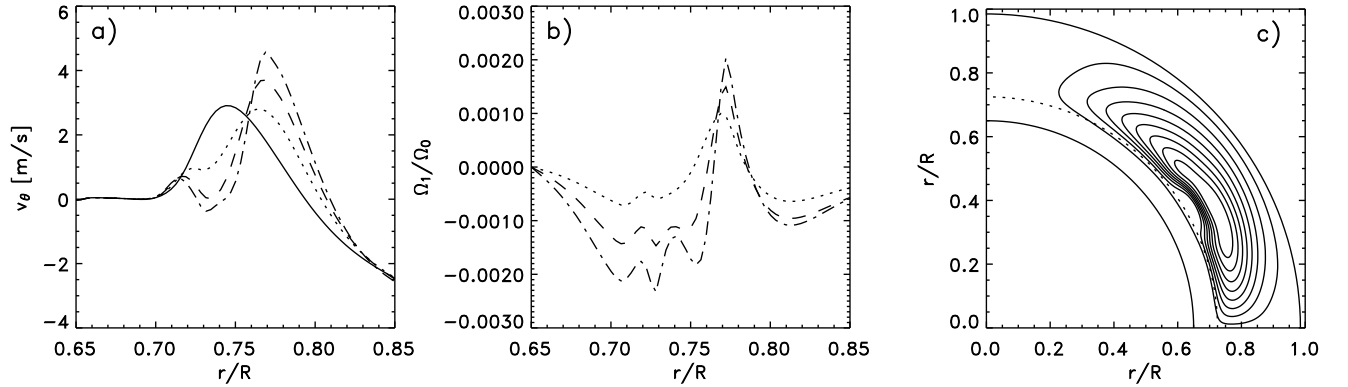


FIG. 6.— Solution with a quenched viscosity. Panel a) shows the meridional flow speed, where the dotted line indicates a quenching by a factor of 2, the dashed line a quenching by a factor of 4, and the dashed-dotted line a quenching by a factor of 8. The solid line indicates the reference solution without any influence of the magnetic field. Panel b) shows the change of differential rotation. Unlike the cases shown in Figs. 2 - 4 there is no formation of a significant jet. Panel c) shows the streamlines for the case with a quenching of the viscosity by a factor of 8.

magnetic flux is not switched off completely in this case. The magnetic field we assumed is centered at $r = 0.75 R_{\odot}$ and has a width of $0.05 R_{\odot}$, which means that the upper half is still in a region of considerable flow speed. For example the effective transport velocity is only reduced by a factor of two when the turbulent viscosity is quenched by a factor of 8).

6. IMPLICATIONS FOR SOLAR DYNAMO MODELS

This investigation shows as a very robust result that the transport capability of the meridional flow is mainly determined by the flow velocity. For a flow velocity of the return flow at the base of the convection zone of about 2.5 m s^{-1} the maximum field strength that can be transported is around 3 T (30 kG). This field strength is found to be rather insensitive to the turbulent viscosity or width of the magnetic band. Inspecting Eq. (16) shows that a larger value for this field strength would require either a very small or a very large value of ν_t/ν_{crit} or a very large value of c_d . Since the meridional return flow is located roughly where ν_t shows the strongest radial gradient at the base of the convection zone the value of ν_t in that region will reflect more convection zone values rather than very small overshoot values. The value of ν_{crit} is mainly influenced through the effective thickness d . Values much larger than the value used in this investigation are not feasible, since then the magnetic layer would have a larger extent in radius than the meridional return flow. For very small values of d an increase in the magnetic field strength that can be transported is expected. This is not too surprising, since for magnetic flux tubes the influence of the drag force is anti proportional to the diameter. Rempel (2003) showed that flux tubes with a diameter of less than 100 km can be transported equatorward even if the field strength is around 10 T, however the magnetic flux associated with these flux tubes is orders of magnitude smaller than the flux of a typical sunspot. We want to emphasize that for flux tubes the use of $c_d \sim Re$ ($c_w = \text{const}$) gives a different scaling of $B \sim v/d^{1/2}$ compared to the $B \sim (\nu_t v)^{1/2}/d$ scaling derived from Eq. (16) in the limit of small values for d .

Feedback through quenching of turbulent viscosity

(also affecting the Λ -effect, which is $\sim \nu_t$ in our model) leads to a significant modification of the meridional flow if the field strength exceeds equipartition. Since typical mixing-length estimates for $B_e q$ at the base of the convection zone are around 1 T, this happens in the same field strength range where the direct feedback through magnetic tension becomes important, too. Therefore if we consider both effects together the effective transport velocities are modified, but the results do not change dramatically.

To summarize, the result that the consideration of the magnetic curvature force limits the magnetic field strength that can be transported towards the equator to about 3 T (30 kG) seems to be very robust within the framework of the mean field model used in this investigation.

Current kinematic solar flux-transport dynamo models rely on the equatorward transport of toroidal field at the base of the convection through the meridional flow (see comparison of solutions with and without meridional flow in Dikpati & Charbonneau (1999); Dikpati & Gilman (2001)). The meridional flow velocity at the base of the convection zone assumed in most of these models is around $1 - 2 \text{ m s}^{-1}$, which is close to the values considered in this paper. That value is also consistent with the observed surface flow of around $10 - 20 \text{ m s}^{-1}$ and a dynamo period around 22 years. The main consequence of the work presented here for flux-transport dynamo models can be summarized as follows: Any field exceeding a few T (10 kG) cannot be transported toward the equator through a meridional flow with an amplitude of a few m s^{-1} . If the solar dynamo produces stronger field (e.g. 100 kG as inferred from studies of rising magnetic flux tubes (Choudhuri & Gilman 1987; Fan et al. 1993; Schüssler et al. 1994; Caligari et al. 1995, 1998)), the field must get amplified locally through induction effects. The stronger field could be in an equilibrium as discussed by Moreno-Insertis et al. (1992); Rempel et al. (2000); Rempel & Dikpati (2003), which would prevent further poleward movement, but an equatorward transport is not possible.

First attempts to include the feedback on meridional flow and differential rotation in a 'dynamic' dynamo

model (Rempel et al. 2005) show that flux-transport dynamos work with toroidal field strengths up to around 30 kG, however additional constraints apply through the observed limits on the amplitude of torsional oscillations (Howe et al. 2004; Rempel et al. 2005), if the feedback on differential rotation is included, too.

The problem addressed in this paper is not limited to flux-transport dynamos. Any dynamo will face the problem that the toroidal field will start moving toward the pole due to the magnetic tension force if the field strength is large enough. If the propagation of the magnetic activity is not an advection effect, but a classic dynamo wave, the wave will have to compete with the poleward movement induced by the magnetic tension force. Since the changes of the meridional flow shown in Fig. 2 are only weakly dependent on the meridional flow speed of the reference state, they also give an estimate how large the poleward movement would be if no meridional flow is present.

We have shown that the formation of a prograde jet is an unavoidable consequence when including the magnetic

tension force. Recently Christensen-Dalsgaard et al. (2004) tried to detect jets associated with toroidal magnetic field in the tachocline. The detection limit they found is of the order of 2 – 4 nHz, which is around 1% of the rotation rate. The jets we see in this study have an amplitude of around 1.5% for the strongest field we considered (4T). Magnetic field of 2T or less leads to the formation of jets with less than 0.5% amplitude. These jets are therefore at or below the detection limit of current helioseismic techniques. If the magnetic field has a more complicated intermittent and also non-axisymmetric structure it is likely that the amplitude of the prograde jet is lower than predicted by our axisymmetric model.

Stimulating discussions and helpful comments on a draft version of this paper by Mausumi Dikpati, Keith MacGregor and Peter Gilman are gratefully acknowledged. The author thanks the anonymous referee for a very helpful review.

REFERENCES

- Braun, D. C. & Fan, Y. 1998, *ApJ*, 508, L105
 Brun, A. S. & Toomre, J. 2002, *ApJ*, 570, 865
 Caligari, P., Moreno-Insertis, F., & Schüssler, M. 1995, *ApJ*, 441, 886
 Caligari, P., Schüssler, M., & Moreno-Insertis, F. 1998, *ApJ*, 502, 481
 Choudhuri, A. R. & Gilman, P. A. 1987, *ApJ*, 316, 788
 Choudhuri, A. R., Schüssler, M., & Dikpati, M. 1995, *A&A*, 303, L29
 Christensen-Dalsgaard, J., Corbard, T., Dikpati, M., Gilman, P. A., & Thompson, M. J. 2004, in *ESA SP-559: SOHO 14 Helio- and Asteroseismology: Towards a Golden Future*, 376–+
 Dikpati, M. & Charbonneau, P. 1999, *ApJ*, 518, 508
 Dikpati, M. & Gilman, P. A. 2001, *ApJ*, 559, 428
 Fan, Y., Fisher, G. H., & DeLuca, E. E. 1993, *ApJ*, 405, 390
 Gilman, P. A. & Miller, J. 1986, *ApJS*, 61, 585
 Glatzmaier, G. A. & Gilman, P. A. 1982, *ApJ*, 256, 316
 Haber, D. A., Hindman, B. W., Toomre, J., Bogart, R. S., Larsen, R. M., & Hill, F. 2002, *ApJ*, 570, 855
 Howe, R., Rempel, M., Christensen-Dalsgaard, J., Hill, F., Komm, R. W., Schou, J., & Thompson, M. J. 2004, in *ESA SP-559: SOHO 14 Helio- and Asteroseismology: Towards a Golden Future*, 468–+
- Küker, M. & Stix, M. 2001, *A&A*, 366, 668
 Kitchatinov, L. L. & Rüdiger, G. 1993, *A&A*, 276, 96
 —. 1995, *A&A*, 299, 446
 Miesch, M. S., Elliott, J. R., Toomre, J., Clune, T. L., Glatzmaier, G. A., & Gilman, P. A. 2000, *ApJ*, 532, 593
 Moreno-Insertis, F., Schüssler, M., & Ferriz-Mas, A. 1992, *A&A*, 264, 686
 Rempel, M. 2003, *A&A*, 397, 1097
 —. 2005, *ApJ*, 622, 1320
 Rempel, M. & Dikpati, M. 2003, *ApJ*, 584, 524
 Rempel, M., Dikpati, M., & MacGregor, K. 2005, *ESA SP-560, CS13 Proceedings*, 913
 Rempel, M., Schüssler, M., & Tóth, G. 2000, *A&A*, 363, 789
 Rüdiger, G., von Rekowski, B., Donahue, R. A., & Baliunas, S. L. 1998, *ApJ*, 494, 691
 Schüssler, M., Caligari, P., Ferriz-Mas, A., & Moreno-Insertis, F. 1994, *A&A*, 281, L69
 Zhao, J. & Kosovichev, A. G. 2004, *ApJ*, 603, 776